JOURNAL OF Materials CHEMISTRY

Synthesis of nanoporous bismuth films by liquid-phase deposition

W.-N. Shen,[a] B. Dunn,*[a] C. D. Moore,[a] M. S. Goorsky,[a] T. Radetic[b] and R. Gronsky[b]

[a]*Department of Materials Science and Engineering, University of California, Los Angeles, CA, 90095-1595, USA. E-mail: bdunn@ucla.edu*
[b]*Department of Materials Science and Mineral Engineering, University of California, Berkeley, CA, 94720-1760, USA*

Received 20th September 1999, Accepted 18th January 2000

A liquid phase deposition method involving metal carboxylates has been used to obtain porous bismuth films. Porous morphologies offer the opportunity to interrupt phonon transport without interfering with electron transport, an important consideration for thermoelectric materials. The films were prepared by spin coating a solution of bismuth(III) 2-ethylhexanoate and 5 wt% glycerol in 2-methylpropan-1-ol with subsequent heat treatment in hydrogen between 250 and 270 °C. Thermal decomposition studies established the intermediate and final products associated with the pyrolysis reaction. The porosity of the resulting films varied from 30 to 50% and residual carbon in the film was removed by hydrogen plasma etching. The pores were present in the form of nano-dimensional channels, on the order of 5–10 nm wide, existing between bismuth grains.

Introduction

Bismuth is one of the most extensively studied thermoelectric materials because of such unique features as a small electron effective mass along the trigonal axis and long electron mean free path.[1] The thermoelectric figure of merit, Z, which is used to characterize thermoelectric materials, is higher for bismuth than any other metal. Z is defined as;[2]

$$Z = \sigma S^2/\kappa \quad (1)$$

where σ is the electrical conductivity, S is the Seebeck coefficient, T is the absolute temperature and κ is the thermal conductivity. The dimensionless parameter, ZT, for bulk single crystalline bismuth parallel to the trigonal direction increases from 0.16 at 100 K to 0.39 at 300 K.[3] The present paper concerns the use of nanoporosity in bismuth films as a strategy for enhancing its value of Z.

Bismuth represents a model system in which to investigate the use of nanoporosity because its electron mean free path (100 to *ca.* 600 nm at 300 K)[4] is much greater than that of the phonon mean free path (18 nm at 300 K).[5] By producing nanometer sized pores with dimensions comparable to the phonon mean free path, there is the likelihood of disrupting phonon transport without seriously affecting electron transport. Thus, the desired microstructure for bismuth is one characterized by a high concentration of pores in the general range of 20 nm; larger pores will lower electron transport while smaller ones are not likely to be as effective in scattering phonons. In research to date, the influence of porosity on thermoelectric properties has been considered in only a few systems, silicon,[6] Si–Ge solid solutions,[7] Al-doped SiC,[8] strontium oxide and strontium carbonate.[9] The pore sizes in most of these studies were in the micrometer range and so no scattering selectivity would be expected. Nonetheless, it is interesting that samples in the Si–Ge alloy system with 15–20% porosity exhibited σ/κ values as much as 30% higher than those of nonporous materials of the same composition.[7] This result suggests that microstructure control of nanoporosity and pore size may offer a novel approach for increasing the thermoelectric figure of merit for appropriate materials.

The present study considers the development of nanoporosity in bismuth thin films. Thin films were selected rather than bulk materials because of the opportunity to use the decomposition of organometallics to produce bismuth with controlled porosity. Several other methods for preparing bismuth thin films have been reported including thermal evaporation,[4,5] molecular beam epitaxy,[1] pulsed laser deposition[10] and sputtering.[11] These studies, however, were directed at producing dense materials. The synthesis approach we have used to obtain nanoporous bismuth is termed metalorganic deposition (MOD).[12] MOD is a nonvacuum, liquid-based technique. Such solution-based methods have become increasingly popular in recent years because of low processing temperatures, environmentally benign conditions and the ability to directly fabricate inorganic films, coatings or fibers.[13,14] In the MOD approach, thin films are deposited from a metalorganic precursor solution by spin-coating. Upon pyrolyzing the bismuth precursor, the organic ligands decompose and release gases, such as carbon dioxide, carbon monoxide and water vapor. Generally, MOD has been used to prepare electrochemical, optical and superconducting inorganic materials.[15–17] However, several metals, including Au, Ag, Cu, Pb and Sn, have also been prepared by MOD.[12]

The present paper describes the use of MOD to prepare thin bismuth films which remain nanoporous because the sintering process has been arrested. In this work the synthesis conditions and heat treatments required to form phase pure porous bismuth with controlled thickness and density are described. An important feature in this work is the use of hydrogen plasma etching to remove residual carbon. Although thermoelectric measurements are not included in this paper, initial results confirm that the basic premises for using nanoporosity are valid. That is, the nanoporous films exhibit a decrease in electrical conductivity,[18] but it is much less than the decrease in thermal conductivity.[19]

Experimental

Metalorganic deposition (MOD) and film synthesis

Bismuth organometallic precursors must not only provide a bismuth source but also possess low volatility and good stability in air so that they may be used under convenient processing conditions. The volatility of precursors is decided by the nature and length of the organic ligands. Metal carbox-

ylates are generally not as volatile and air sensitive as metal alkyls or metal alkoxides. The relative volatility for Bi precursors is:

$$BiR_3 > Bi(OR)_3 > Bi(OOCR)_3 \quad (2)$$

where R represents a saturated hydrocarbon group (*e.g.* for bismuth carboxylates, CH_3 for bismuth(III) acetate or $CH(C_2H_5)C_4H_9$ for bismuth(III) 2-ethylhexanoate). Longer organic chain precursors exhibit lower volatility, however, they are more likely to lead to higher levels of residual carbon in the films after pyrolysis. The nature of the organic ligand is quite important as this is the species responsible for producing pores within the bismuth films. During pyrolysis of the metalorganic precursors, the organic ligands are decomposed to release gases (CO, CO_2, H_2O) which create the porosity in the film. Owing to the low melting temperature of bismuth (mp 271 °C), the temperature range for the thermal decomposition reactions should be at or below the bismuth melting point in order to control porosity in the final film. The studies reported here are based on the use of the bismuth carboxylate precursor, bismuth(III) 2-ethylhexanoate. A few supplemental studies are reported using bismuth(III) acetate.

Bismuth(III) 2-ethylhexanoate (BiEH) and bismuth(III) acetate (BiAc) were obtained from Alfa Aesar (both 99.99%). Before mixing, BiEH was dried under vacuum to remove residual 2-ethylhexanoic acid. The solvent system was 2-methylpropan-1-ol with 5 wt% glycerol added to improve wetting characteristics (both 99.5% from Aldrich). A homogeneous solution of the precursor was prepared and filtered. The concentration of the BiEH was adjusted from 36 to 70 wt%. The solution was then spin-coated on Si(100), Pyrex or other substrates (*ca.* 50 mm × 50 mm) with the optimum conditions being a rotation speed of 4000 rpm for 30 s. After spin-coating, the films were placed in a quartz tube and heated in a furnace at either 250 or 270 °C in flowing ultra pure hydrogen (99.999%). Before the reaction, the tube was pumped down to <100 mTorr and then Ar gas was used to purge the tube prior to filling with hydrogen gas. The heating time was generally 3 or 6 h with a 20 °C min^{-1} ramp rate. To limit the exposure of the porous bismuth films to air, the films were stored in an Ar-filled chamber.

After pyrolysis, the porous bismuth films were subjected to a hydrogen plasma etching treatment.[20] This treatment was designed to remove residual carbon and oxygen from the films as these species can have a profound effect on transport properties. The plasma source gas was a mixture of 10% H_2 and 90% N_2. The plasma generator (Opthos Instruments, Inc) operated at 2.45 GHz. Experiments showed that with a 30 mTorr source gas pressure, a 10 W hydrogen plasma for 30 s was optimal for removing residual carbon from porous bismuth films deposited on Pyrex substrates. For Si(100) substrates, a 6 W plasma for 25 s was used.

Characterization methods

A variety of methods were used in characterizing two different features of this study; the thermal decomposition reactions which are of central importance in determining film synthesis conditions and the microstructural properties of the final film. The thermal decomposition studies used a combination of thermogravimetric analysis (TGA; Texas Instruments), FTIR (Perkin-Elmer) and X-ray diffraction (XRD; Rigaku). The thicknesses of the porous bismuth films were determined using profilometry (Tencor Alpha-step). The corners of the bismuth films were etched by concentrated nitric acid to expose the substrate surface and create the step required for the measurement. Repetitive measurements indicated the uncertainty in film thickness was ±10%. Film microstructure was determined by transmission electron microscopy (TEM) using a JEOL 200CX microscope. The TEM specimens were ion-milled (Gatan) at 77 K from the substrate side. A software package (Prism; Analytical Vision, Inc.) was used to analyze images from the TEM for grain size distribution. Auger depth profiling was carried out using a Physical Electronics system.

Film porosity was measured by an X-ray reflectivity technique.[21] The measurement is non-destructive, requires no sample preparation and is sensitive to amorphous as well as crystalline materials. Average values of film density are obtained along with quantitative information concerning surface roughness. The measurements were made on a modified Bede D^3 diffractometer, using Cu-Kα radiation, a two bounce Si(111) collimator and one bounce Si(111) monochromator. As the angle between the surface and the X-ray beam increases, the beam undergoes total external reflection until it reaches the critical angle where the X-rays penetrate the surface. Beyond this angle the intensity collected is determined by the roughness of the surface, with smooth samples showing a decrease in intensity proportional to θ^{-4}, and rough samples showing a steeper gradient. The film density is derived from the critical angle from the following equation:

$$\theta_c = \lambda\left(\frac{N_A r_o}{\pi}\sum_j \frac{\rho_j}{A_j}\,(Z_j + f_j)\right)^{1/2} \quad (3)$$

where θ_c is the critical angle, N_A is Avogadro's number, r_o is the classical electron radius, ρ_j is density, A_j is the atomic mass, Z_j is the atomic number, f_j is a form factor and λ is the photon wavelength. The experimental data has been matched with a simulated scan to improve the accuracy of measurement. Once the film density is determined, the film porosity, P, is calculated from:

$$P = 1 - (\rho/\rho_o) \quad (4)$$

where ρ_o is the density of bulk bismuth (9.80 g cm^{-3} at 300 K).[22]

Results and discussion

Synthesis of porous bismuth films

The MOD solution for synthesizing porous bismuth films is based on dissolving the BiEH into 2-methylpropan-1-ol. This system exhibits excellent solubility and homogeneous solutions were prepared with as much as 70 wt% BiEH added. Several other solvent systems were examined including xylene, 2-methoxyethanol and 2-ethylhexanoic acid. The 2-methylpropan-1-ol solvent system in combination with the additive glycerol offers the best film quality. The glycerol addition not only increases solution viscosity and wettability on various substrates, but also improves film densification and reduces film roughness. Glycerol possesses higher viscosity than most organic solvents and its high boiling point (bp 290 °C) slows the evaporation rate of the solvent system.

The wettability of this precursor solution on various substrates is excellent. The substrates examined include Pyrex, Si(100), Kapton, polycrystalline MgO and polycrystalline Al_2O_3. Without glycerol, the Pyrex surface is too smooth (roughness about 6 nm) to provide adequate wettability for the precursor solutions. To overcome this wetting problem, the Pyrex substrates were pretreated by reactive ion etching (RIE) using a gas mixture of CF_4 and O_2. The addition of glycerol wets the Pyrex so effectively that no RIE is required to produce highly uniform films.

The decomposition characteristics of BiEH and BiAc were studied in some detail as this information provides appropriate guidance for developing heat treatments that produce porous bismuth. These studies bring forth two important features associated with these carboxylate precursors; (a) bismuth oxide forms even in N_2 and (b) it is feasible to fully decompose the

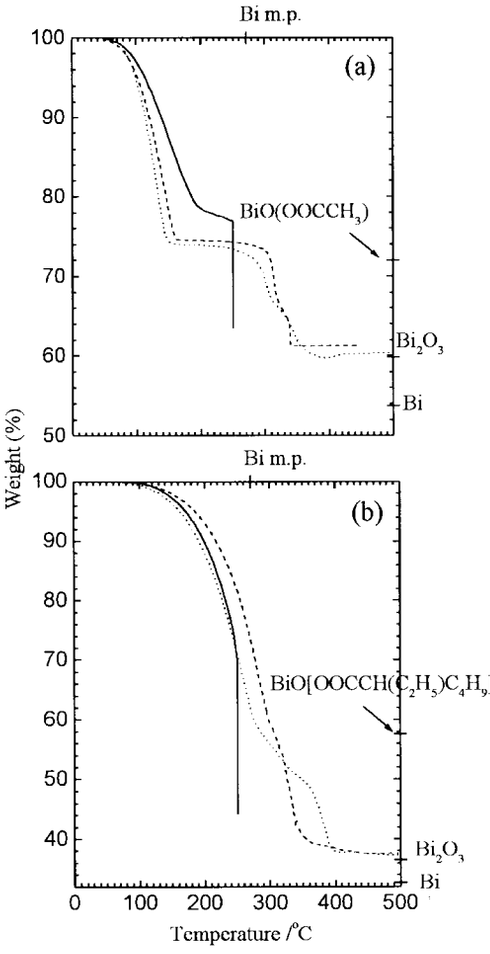

Fig. 1 Thermogravimetric analysis results for (a) bismuth(III) acetate (BiAc) and (b) bismuth(III) 2-ethylhexanoate (BiEH). The ramping rate is 10 °C min^{-1}. Heat treatments are under N_2 (·····) or air (- - - -). The solid line shows the experiment where the reaction is held at 250 °C for 15 h under 10% H_2 in He (—). The labels on the right hand side represent the theoretical weight losses for Bi precursors to transform into the different compounds.

bismuth precursors at temperatures below 250 °C provided there is sufficient reaction time.

The decomposition of BiAc has been reported previously.[23] A two-stage decomposition mechanism was identified involving the formation of a bismuth oxide acetate intermediate, $BiO(OOCCH_3)$.

$$2\ Bi(OOCCH_3)_{3(s)} \xrightarrow{\text{heat}} 2\ BiO(OOCCH_3)_{(s)} + 2\ O(COCH_3)_{2(g)} \quad (5)$$

$$2\ BiO(OOCCH_3)_{(s)} \xrightarrow{\text{heat}} \beta\text{-}Bi_2O_{3(s)} + O(COCH_3)_{2(g)} \quad (6)$$

Our TGA results [Fig. 1(a)] are consistent with this mechanism. In the range 100–150 °C, BiAc starts to decompose into bismuth oxide acetate, $BiO(OOCCH_3)$ [eqn. (5)]. In addition to the TGA measurements, X-ray diffraction (not shown here) was used to confirm its presence. This intermediate compound remains stable until 300 °C when it becomes β-Bi_2O_3 in the final step at 350 °C [eqn. (6)]. Acetates are known to decompose to give acetone and CO_2,[24] however, our mass spectrometry results for these products were inconclusive.

The experiments with BiAc indicate that in flowing N_2, the carboxylate ligand itself serves as the oxygen source in forming the bismuth oxide.[23] Thus, it is necessary to heat the bismuth precursor in a reducing atmosphere (*e.g.* H_2) in order to obtain metallic bismuth. When BiAc was reduced in pure H_2, the last

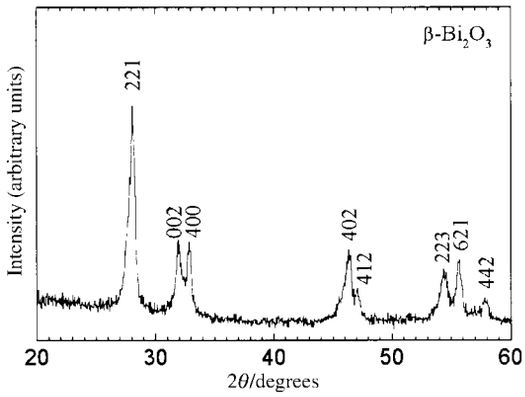

Fig. 2 X-Ray diffraction for bismuth(III) acetate heated at 250 °C under 10% H_2 in He for 30 h. The peaks are indexed to β-Bi_2O_3.

step of the decomposition reaction becomes eqn. (7) rather than eqn. (6):

$$2\ BiO(OOCCH_3)_{(s)} + 3\ H_{2(g)} \xrightarrow{\text{heat}} 2\ Bi_{(s)} + O(COCH_3)_{2(g)} + 3\ H_2O_{(g)} \quad (7)$$

This decomposition [eqn. (7)] will occur when the reaction is held sufficiently long even at low temperature (250 °C) [Fig. 1(a)]. If the environment is not sufficiently reducing, β-Bi_2O_3 is produced as shown in Fig. 2 for a sample heated in 10% H_2 (in He). All the solid products indicated in eqns. (5)–(7) were identified using XRD and TGA.

Similar TGA studies have been applied to BiEH [Fig. 1(b)]. As observed with BiAc, a two-stage decomposition process is suggested for thermal decomposition of BiEH in air or N_2 as shown in eqns. (8) and (9). The TGA measurements show that BiEH begins to decompose around 100 °C and the final step occurs in the range 350–400 °C range.

$$2\ Bi[OOCCH(C_2H_5)C_4H_9]_{3(l)} \xrightarrow{\text{heat}} 2\ BiO[OOCCH(C_2H_5)C_4H_9]_{(s)} + 2\ O[OCCH(C_2H_5)C_4H_9]_{2(g)} \quad (8)$$

$$2\ BiO[OOCCH(C_2H_5)C_4H_9]_{(s)} \xrightarrow{\text{heat}} \beta\text{-}Bi_2O_{3(s)} + O[OCCH(C_2H_5)C_4H_9]_{2(g)} \quad (9)$$

Once again, by using pure H_2, pure bismuth is formed rather than β-Bi_2O_3 as shown in eqn. (10).

$$2\ BiO[OOCCH(C_2H_5)C_4H_9]_{(s)} + 3\ H_{2(g)} \xrightarrow{\text{heat}} 2\ Bi_{(s)} + O[OCCH(C_2H_5)C_4H_9]_{2(g)} + 3\ H_2O_{(g)} \quad (10)$$

The intermediate product, bismuth oxide 2-ethylhexanoate, $BiO[OOCCH(C_2H_5)C_4H_9]$, is suggested from both TGA [Fig. 1(b)] and FTIR (Fig. 3). The spectrum in Fig. 3(b) and especially the peak for ν(BiO) around 550 cm^{-1} are consistent with that reported for another oxo–bismuth carboxylate, BiO(OOCH).[25] Interestingly, this compound was identified as the intermediate in the thermal decomposition of still another bismuth carboxylate, $Bi(OOCH)_3$.

The films require at least 1 h at temperatures above 250 °C in H_2 to show complete conversion to metallic bismuth. During the heat treatment, sintering also occurs so that the thickness of the bismuth film decreases as a function of heating time. XRD shows that the resulting films are polycrystalline with some preferred orientation (Fig. 4). Films heated for <3 h exhibited an orientation in which the (012) plane was parallel to the bismuth film surface. After 6 h, a trigonal orientation, which is common for bismuth films,[4,11] was evident.

Film thickness is determined by several factors including

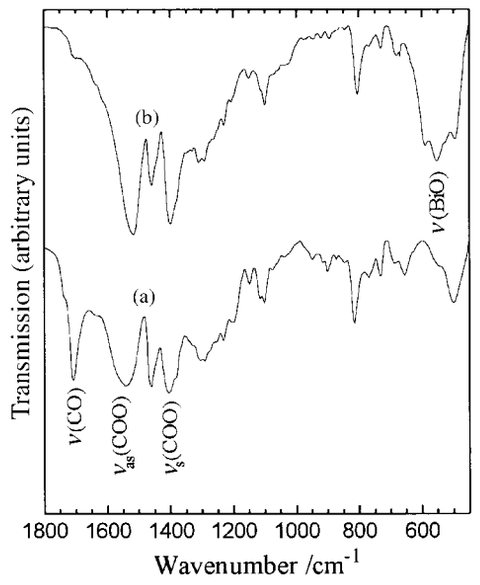

Fig. 3 FTIR spectra for (a) bismuth(III) 2-ethylhexanoate ($Bi[OOCCH(C_2H_5)C_4H_9]_3$) and (b) bismuth(III) oxide 2-ethylhexanoate ($BiO[OOCCH(C_2H_5)C_4H_9]$). Vibrational peaks around 1400 cm^{-1}, $\nu_s(COO)$, and 1530 cm^{-1}, $\nu_{as}(COO)$, represent bismuth carboxylates.[23,24] The peak at 1700 cm^{-1} belongs to the residual 2-ethylhexanoaic acid which disappears after heating to 260 °C. The extra peak $\nu(BiO)$ at around 550 cm^{-1} is evidence for the formation of bismuth(III) oxide 2-ethylhexanoate.

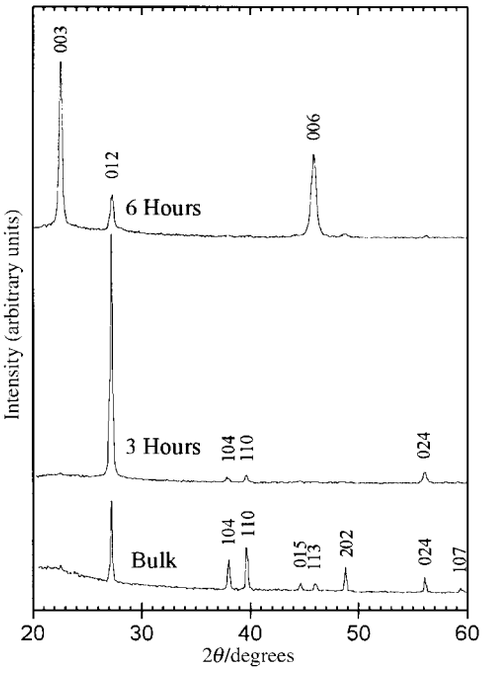

Fig. 4 X-Ray diffraction results for porous bismuth thin films obtained using 43 wt% BiEH heated at 250 °C. Results are compared to bulk bismuth. Heating times are labeled individually.

precursor solution concentration, solution viscosity, heat treatment conditions, spin-coating rotation speed and substrate wettability. In general, the thickness of the porous bismuth film is controlled from 40 to nearly 600 nm by varying the solution concentration and sintering conditions [Fig. 5(a) and Table 1]. The films are quite uniform in thickness as the film color and appearance are unchanged across the entire substrate. The more dilute precursor solutions (43 wt% BiEH) with longer heating times (6 h at 250 °C) led to a film thickness of 80 nm. Increasing the sintering temperature to 270 °C further reduced

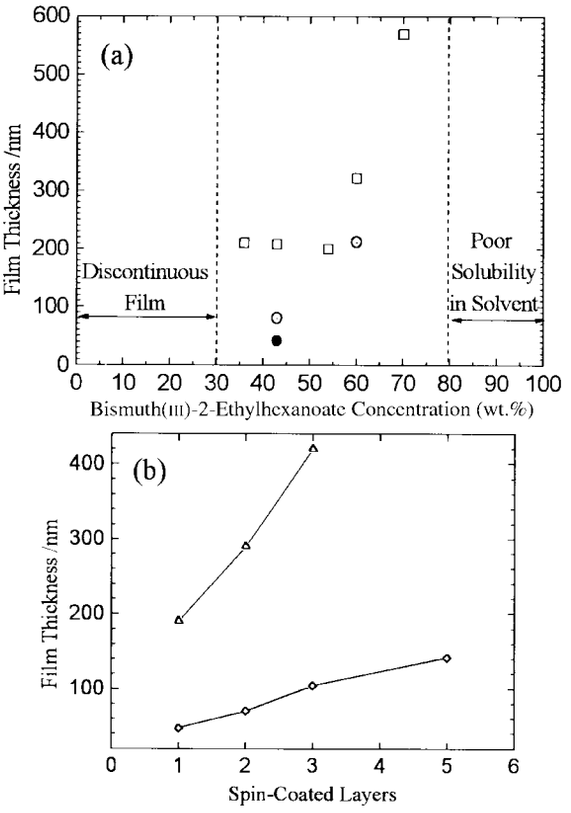

Fig. 5 Thickness of spin-coated porous Bi thin films. (a) Single layer deposition; samples heated at 250 °C for 3 h (□) and 6 h (○) and at 270 °C for 6 h (●). Solution concentrations of <30 wt% result in discontinuous films while concentrations >80 wt% are insoluble. (b) Multiple layer deposition; samples heated at 270 °C for 6 h. Films were obtained from 43 wt% (◊) and 60 wt% BiEH solutions (△), respectively.

the thickness to 40 nm. More concentrated BiEH solutions produced thicker bismuth films owing to the higher viscosity of the precursor solution. Another method of producing thicker films is to spin-coat multiple layers of the precursor solution prior to the pyrolysis treatment. To avoid the formation of interfaces between successive layers, precursor films were dried for 2 min in flowing air to accelerate the evaporation of excess solvent before depositing the next layer. Bismuth films containing as many as five layers were prepared by this process [Fig. 5(b)].

Hydrogen plasma etching

Auger measurements indicated the presence of carbon (4 wt%) and oxygen (2 wt%) in the porous bismuth thin films (the error limits for these measurements are ±10%). Residual carbon comes from the incomplete decomposition of the BiEH organic ligands; oxidation occurs simply from exposing the film to air for prolonged periods of time. One important reason for removing residual carbon from the bismuth film is that its presence may lead to low values of the electrical conductivity. From the plasma etching process described here, the electrical conductivity for the porous Bi films increased by nearly 1000 times, from 0.2 to 150 Ω^{-1} cm^{-1} at room temperature.[18] Selected transport properties for plasma-etched films are listed in Table 2. In addition to removing residual carbon, the larger grain size caused by plasma etching (*vide infra*) is another factor which can improve conductivity.

The composition profile obtained from the Auger measurements indicated that the hydrogen plasma etching process removed carbon from the top half of the film. The bottom half of the film (closest to the substrate) was not affected by the

Table 1 Process conditions for porous bismuth films

Precursor concentration/wt%	Pyrolysis temperature/°C	Sintering time/h	Layer(s)	Film thickness/nm	Porosity (%)	Grain size[a]/nm
36	250	3	1	210		
43	250	3	1	210	50	
		6	1	80	30	
		12	1	70		
	270	6	1	40	30	34
			2	70	33	31
			3	100	38	32
			5	140	35	29
	270	6	1[b]	60	32	36
54	250	3	1	200		
60	250	3	1	320	45	
		6	1	210	42	
	270	6	1	190		
			2	290		
			3	420		
70	250	3	1	570		

[a]Grain size determined from X-ray data of the (003) reflection by the Scherrer equation.[26] [b]Film treated by hydrogen plasma etching after pyrolysis.

Table 2 Electrical properties of plasma-etched bismuth films[a]

	Temperature/K	
	300	100
Electrical conductivity/S cm^{-1}	150	95
Seebeck coefficient/μV K^{-1}	−50	−30

[a]Film thickness: 60 nm; film porosity: 32%.

etching. Thus, after the H_2 plasma treatment, there is a gradient in carbon content across the film, from 2 wt% near the surface to 4 wt% close to the substrate. After etching, the average carbon and oxygen contamination levels become 3 wt% and 2 wt% respectively. In addition, XRD shows that the hydrogen plasma etching process is successful in removing some oxide impurity (β-Bi_2O_3). XRD also indicates that hydrogen plasma etching does not affect the trigonal orientation of the bismuth films.

Film microstructure

The use of X-ray reflectivity provides a non-destructive method for determining film density.[21] In general, film density follows a pattern similar to film thickness in that larger precursor concentrations, higher heat treatment temperatures and longer heating times lead to denser films. For the porous bismuth films discussed here, film porosity was controlled from 30 to 50% (Table 1). H_2 plasma etching has a relatively small effect on film porosity. The X-ray reflectivity curves in Fig. 6 indicate that there is a slight increase in porosity by the etching process, from 30 to 32%.

The TEM images indicate the manner by which porosity is distributed in the MOD prepared films (Fig. 7). The microstructure consists of nanoporous channels (average pore width of 5–10 nm) interspersed between polygonal faceted crystallites [Fig. 7(a)]. The existence of nanoporous channels and polygonal shaped grains [average grain size *ca.* 30 nm in Fig. 7(a)] for these porous bismuth films is distinctly different from columnar microstructures reported for thermally deposited bismuth films.[4] After H_2 plasma etching, the bismuth films undergo an interesting morphological change. The pore channels become wider (to 30 nm) and the grain size increases to *ca.* 90 nm. It is evident that some grains exhibit convoluted shapes and that subgrains have agglomerated to form larger grains [Fig. 7(b)] with a wide grain size distribution. Applying the Scherrer equation[26] to the XRD data, an average grain size (29–36 nm) along (003) was calculated for both plasma treated and untreated samples (Table 1). This value is consistent with

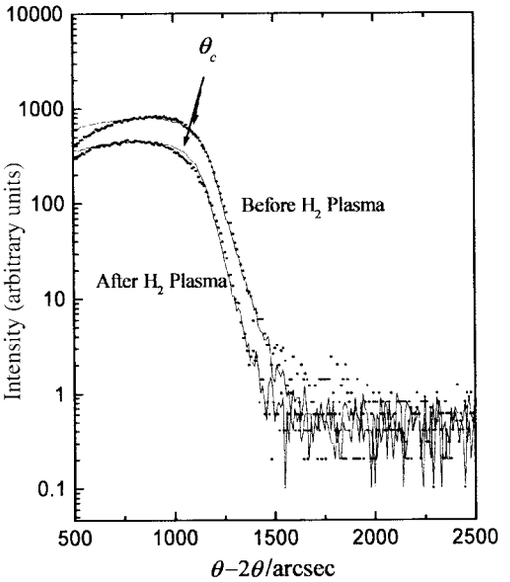

Fig. 6 X-Ray reflectivity data for bismuth thin films heated at 270 °C for 6 h before and after plasma etching. The value of θ_c is used to determine the film density. The dots (•) represent the experimental data; lines (—) represent the simulation results.

that obtained from the TEM image for the sample which was not plasma etched [Fig. 7(a)] and offers further evidence of subgrain agglomeration for the plasma treated sample [Fig. 7(b)]. The existence of subgrains within large grains may be from the redeposition of bismuth on the film surface which is caused by the plasma etching process. The porosity and average grain size for single layer films are virtually the same as for thicker films prepared by multiple layer deposition (Table 1).

Conclusion

Nanoporous bismuth films have been prepared using a MOD process based on dissolving bismuth 2-ethylhexanoate into 2-methylpropan-1-ol with glycerol addition. The addition of glycerol improved the wettability on different substrates and reduced film roughness. Thermal decomposition studies have been carried out for both bismuth acetate and bismuth 2-ethylhexanoate. Pyrolysis in pure hydrogen is necessary to fully convert the bismuth carboxylate precursors to metallic bismuth. The residual carbon in the films is effectively lowered by hydrogen plasma etching.

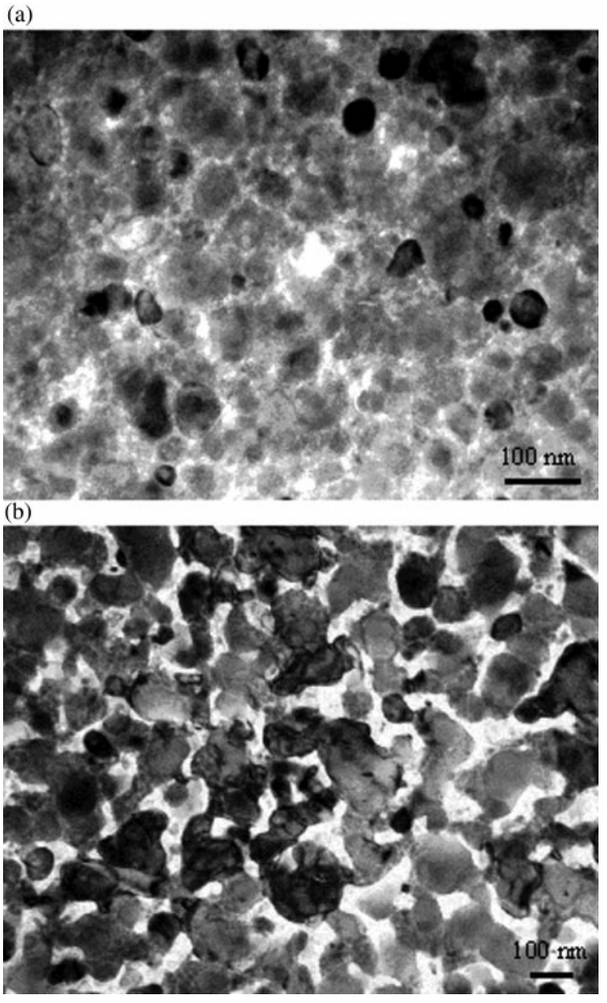

Fig. 7 Plan view TEM images for porous bismuth films. Films were heated at 270 °C for 6 h. The dark area represents bismuth grains, the gray area indicates pores. (a) Prior to H_2 plasma etching; the average pore channel width is 5–10 nm and the mean grain size is 31 nm. (b) After H_2 plasma etching; the average channel pore size is 30 nm wide and the mean grain size is 89 nm.

The microstructure developed in the porous bismuth film from the MOD process is considerably different from that reported for other bismuth thin film approaches. Nanoporous channels on the order of 5–10 nm wide (somewhat wider in the plasma processed film) exist between grains of bismuth. This microstructure is the type desired for increasing the thermoelectric figure of merit. The average pore diameter for both the untreated and plasma treated films is of the same magnitude as the phonon mean free path. The importance of this microstructure in lowering the thermal conductivity of bismuth has been reported[19] and experiments directed at determining the *ZT* values of these films are in progress.

Acknowledgements

The authors greatly appreciate the support of the research under DOD/ONR MURI program on thermoelectrics (N00014-97-1-0516). TEM was carried out at the National Center for Electron Microscopy at the Lawrence Berkeley National Laboratory. The authors also thank Dr H. P. Gillis (UCLA) for his help with hydrogen plasma etching and both Dr Leslie Momoda and John Vajo (Hughes Research Laboratory) for the Auger measurements. The assistance of Dr. A. C. Ehrlich and Dr. W. Fuller-Mora of the Naval Research Laboratory in carrying out transport measurements is greatly appreciated.

References

1 C. A. Hoffman, J. R. Meyer, F. J. Bartoli, A. Di Venere, X. J. Yi, C. L. Hou, H. C. Wang, J. B. Ketterson and G. K. Wong, *Phys. Rev. B*, 1993, **48**, 11431.
2 D. M. Rowe, in *CRC Handbook of Thermoelectrics*, CRC Press, Boca Raton, FL, 1995, p. 2.
3 C. F. Gallo, B. S. Chandrasekhar and P. H. Sutter, *J. Appl. Phys.*, 1967, **34**, 144.
4 P. Mikolajczak, W. Piasek and M. Subotowicz, *Phys. Status Solidi A*, 1974, **25**, 619.
5 F. Völklein and E. Kessler, *Thin Solid Films*, 1986, **142**, 169.
6 G. Gesele, J. Linsmeier, V. Drach, J. Fricke and R. Arens-Fischer, *J. Phys. D: Appl. Phys.*, 1997, **30**, 2911.
7 N. S. Lidorenko, O. M. Narva, L. D. Dudkin and R. S. Erofeev, *Inorg. Mater.*, 1970, **6**, 1853.
8 K.-F. Cai, J.-P. Liu, C.-W. Nan and X.-M. Min, *J. Mater. Sci. Lett.*, 1997, **16**, 1876.
9 H. Szelagowski, I. Arvanitidis and S. Seetharaman, *J. Appl. Phys.*, 1999, **85**, 193.
10 M. O. Boffoué, B. Lenoir, H. Scherrer and A. Dauscher, *Thin Solid Films*, 1998, **322**, 132.
11 A. V. Wagner, R. J. Foreman, L. J. Summers, T. W. Barbee and J. C. Farmer, *Proc. 16th Int. Conf. Thermoelectr.*, 1995, p. 283.
12 J. V. Mantese, A. L. Micheli, A. H. Hamdi and R. W. Vest, *MRS Bull.*, 1989, **14**, 48.
13 D. Segal, *J. Mater. Chem.*, 1997, **7**, 1297.
14 F. F. Lange, *Science*, 1996, **273**, 903.
15 S. Xue, W. Ousi-Benomar and R. A. Lessard, *Thin Solid Films*, 1994, **250**, 194.
16 G. Braunstein, G. R. Paz-Pujalt, M. G. Mason, T. Blanton, C. L. Barnes and D. Margevich, *J. Appl. Phys.*, 1993, **73**, 961.
17 L. S. Hung and D. K. Chatterjee, *J. Mater. Res.*, 1991, **6**, 459.
18 W.-N. Shen, B. Dunn, F. Ragot, M. S. Goorsky, C. D. Moore, G. Chen, R. Gronsky, W. W. Fuller-Mora, D. J. Gillespie and A. C. Ehrlich, *Mater. Res. Soc. Symp. Proc.*, 1999, **545**, 273.
19 D. W. Song, W.-N. Shen, T. Zeng, W. Liu, G. Chen, B. Dunn, C. D. Moore, M. S. Goorsky, T. Radetic and R. Gronsky, *Proc. ASME Heat Transfer Div.*, 1999, **364-1**, 345.
20 G. S. Sandhu, *US Pat.*, 5691009, 1997.
21 C. D. Moore, T. P. A. Hase and B. K. Tanner, *Adv. X-ray Anal.*, 1997, **40**, 113.
22 *CRC Handbook of Chemistry and Physics*, ed. R. C. Weast, CRC Press, Boca Raton, FL, 1981, p. B-82.
23 A. P. Pisarevskii and L. I. Martynenko, *Russ. J. Coord. Chem.*, 1994, **20**, 303.
24 R. Leibold and F. Huber, *J. Thermal Anal.*, 1980, **18**, 493.
25 V. G. Gattow and K. Sarter, *Z. Anorg. Allg. Chem.*, 1980, **468**, 163.
26 B. D. Cullity, *Elements of X-Ray Diffraction*, Addison-Wesley, London, 1978, p. 102.

Paper a907581j